Supplementary Information

Modulating the Alkalinity of Molten Chloride Salt with Proton Sources for Ammonia Synthesis

Bingxu Xi,[1] Jian Liu,[1] Bo Yang,[1] and Xiaofei Guan[1,] *
[1] School of Physical Science and Technology, ShanghaiTech University, Shanghai, 393 Huaxia Middle Road, Shanghai, 201210, China
*E-mail: guanxf@shanghaitech.edu.cn; xiaofei@bu.edu

Contents:

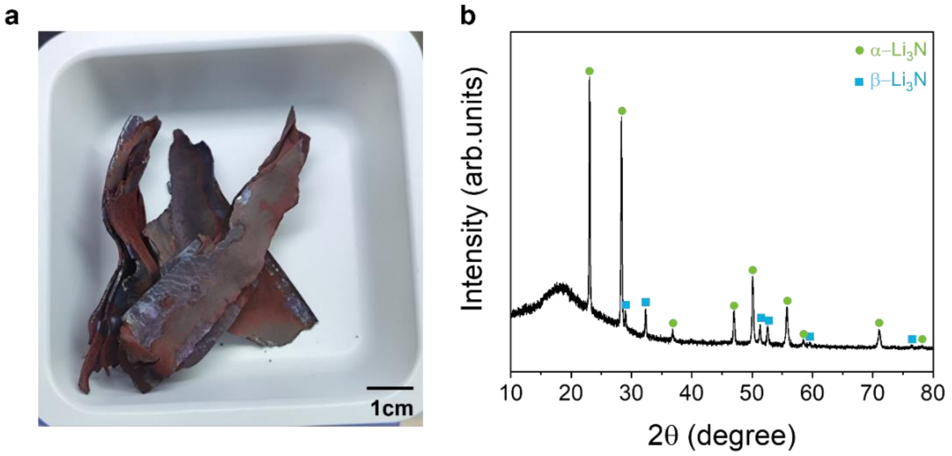

Figure S1. (a) A digital photograph of the Li_3N prepared from the reaction between Li metal and N_2 at 100 ºC for 24 h. (b) The XRD pattern of the Li_3N product. The characteristic peaks for *α*-Li_3N (PDF card No. 76-0593) and *β*-Li_3N (PDF card No. 78-2005) were indexed. The wide signal at around 18º was attributed to the polyimide film cover for the sample.

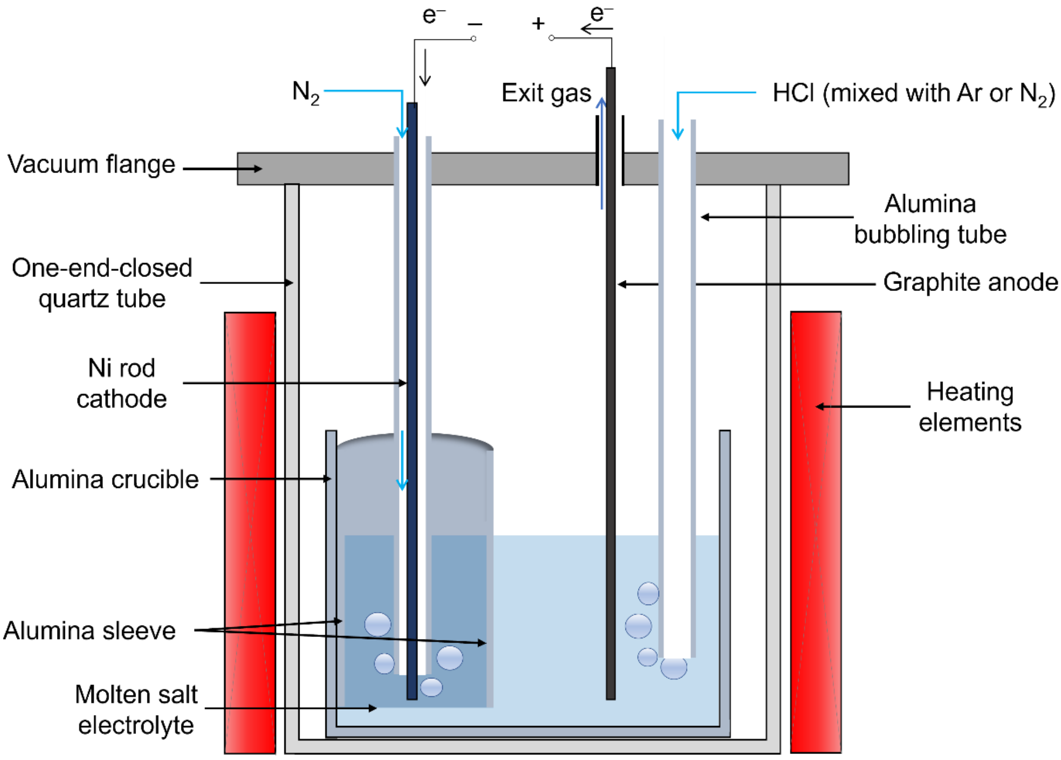

Figure S2. Schematic diagram of the setup of the 3-step experiment for NH_3 synthesis. During the 1 h electrolysis, metallic Li generated was confined within an alumina sleeve. Subsequently, N_2 was introduced into the cathode region for two hours to react with the Li, forming Li_3N dissolved as Li^+ and N^{3-} in the molten salt. The N^{3-} ions diffused throughout the molten salt and ultimately reacted with the HCl introduced in the third step to generate NH_3.

Table S1. Amount of NH_3 absorbed in the reactors containing molten salts of varying compositions. In each experiment, 5at%NH_3–95at%Ar was introduced into the reactor at 20 cm^3/min for 6 h at 500 ºC. An empty reactor was used in the baseline experiment.

Experiments	**Mass of NH_3 in the exit gas over 6 h (g)**	**Total mass of NH_3 absorbed (g)**	**Total moles of NH_3 absorbed (mol)**
Empty reactor	0.2058	0	0
LiCl–KCl	0.1912	0.0146	8.590×10^{-4}
0.002 mol LiH–LiCl–KCl	0.1809	0.0249	1.465×10^{-3}
0.004 mol LiH–LiCl–KCl	0.1444	0.0614	3.612×10^{-3}
0.006 mol LiH–LiCl–KCl	0.1422	0.0636	3.741×10^{-3}
0.008 mol LiH–LiCl–KCl	0.1067	0.0991	5.829×10^{-3}
0.002 mol Li_3N–LiCl–KCl	0.1547	0.0511	3.006×10^{-3}
0.004 mol Li_3N–LiCl–KCl	0.1116	0.0942	5.541×10^{-3}
0.006 mol Li_3N–LiCl–KCl	0.0556	0.1502	8.835×10^{-3}
0.008 mol Li_3N–LiCl–KCl	0.0176	0.1882	1.107×10^{-2}

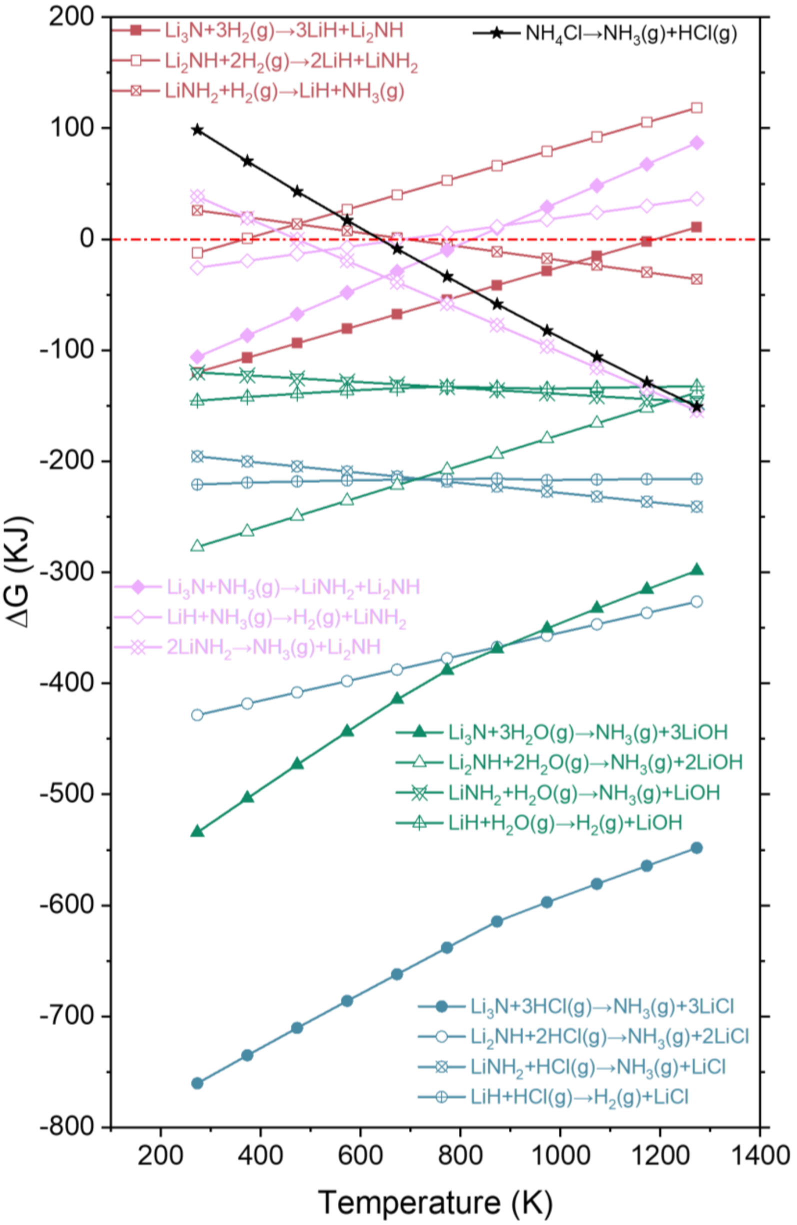

Figure S3. The temperature dependence of the change in Gibbs free energy changes for the reactions involved in the experiments. The values of the enthalpies of $LiNH_2$ and Li_2NH are taken from the literature.[1] The enthalpies and entropies of other substances are taken from "Standard Thermodynamic Properties of Chemical Substances" published by NIST. The enthalpy changes and the entropy changes of the reactions were assumed to be independent on temperature. The standard molar enthalpy of formation and standard molar entropy of each substance were used in the calculations.

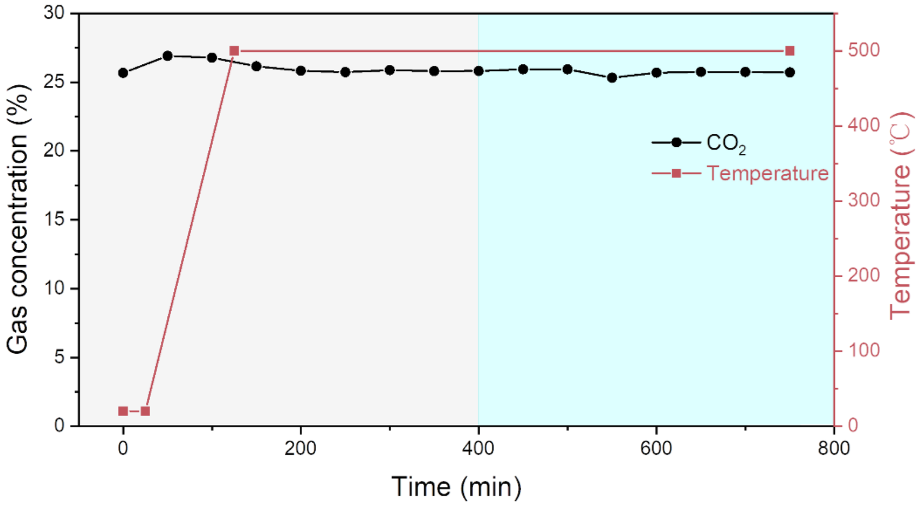

Figure S4. Time dependence of the temperature and the CO_2 concentration detected by GC in the experiment of introducing 25%CO_2–75%Ar to the molten LiCl–KCl.

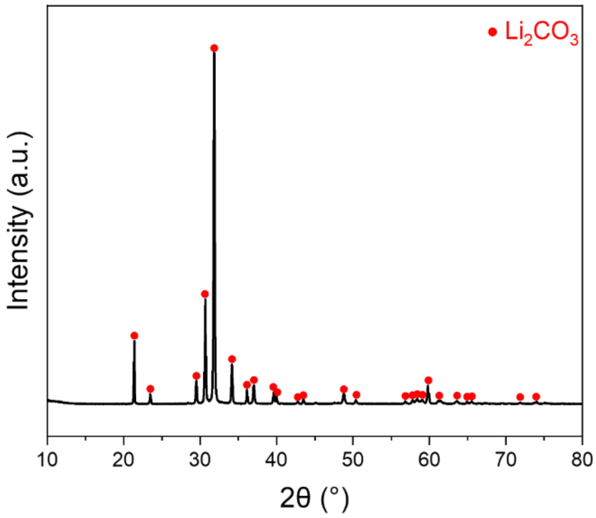

Figure S5. The XRD pattern of the solid white powders obtained after washing the salt (resulting from the reaction between 25%CO_2–75%Ar and 5mol% Li_3N in molten salt) with de-ionized water and drying it. The XRD pattern shows Li_2CO_3 (PDF card No. 87-0729) as the dominant phase.

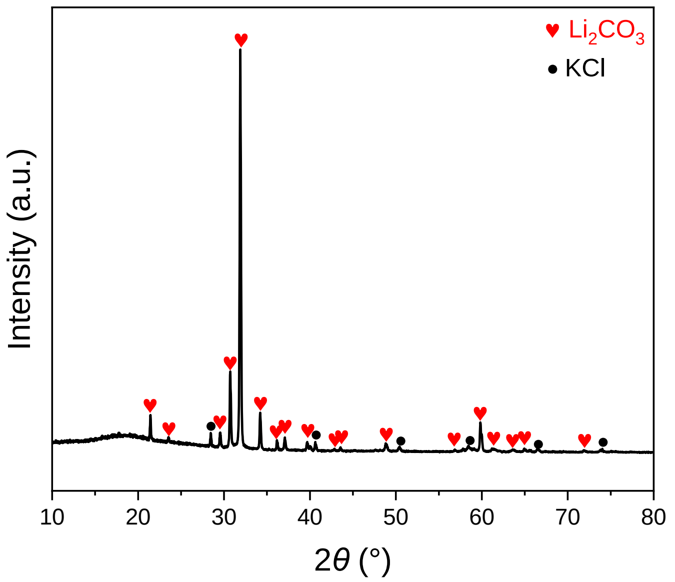

Figure S6. The XRD pattern of the solid white powders obtained after washing the salt (resulting from the reaction between 25%CO_2–75%Ar and 5mol% LiH in molten salt) with de-ionized water and drying it. The XRD pattern shows the Li_2CO_3 (PDF card No. 87-0729) as the dominant phase and the KCl (PDF card No. 72-1540) as the minor phase.

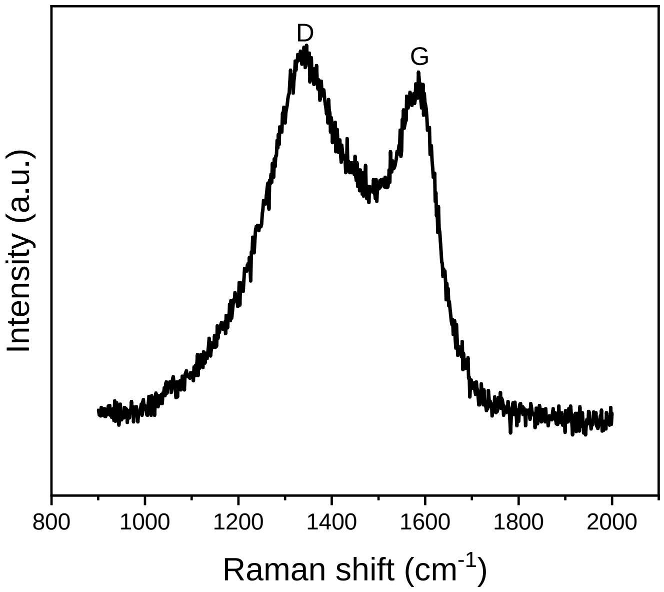

Figure S7. Raman characterization of the black solid sample collected from the upper part of the reactor after the reaction between CO_2 and LiH in the molten salt. Before the Raman characterization, the sample was washed with deionized water and ethanol and subsequently dried.

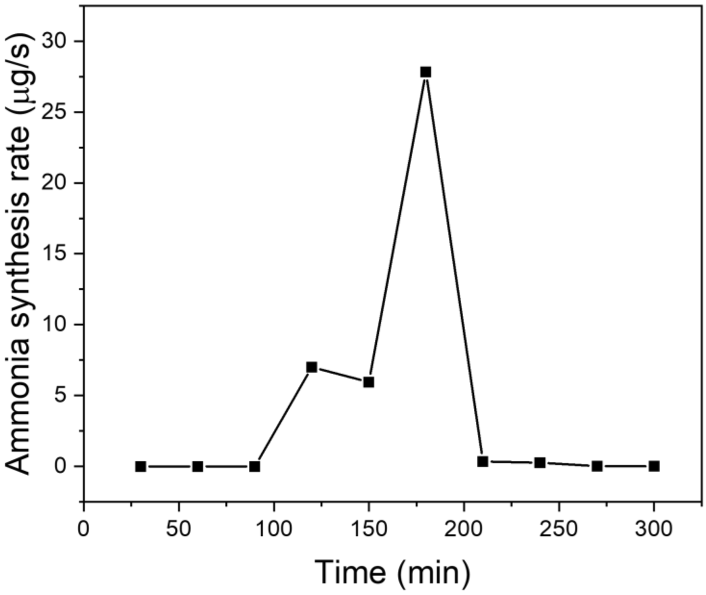

Figure S8. The time dependence of the NH_3 yield rate obtained in the experiment of introducing H_2O carried by Ar to the molten eutectic LiCl–KCl containing 2 mol% of Li_3N. To prepare the salt, ~7.8771 g of LiCl, ~9.7068 g of KCl were weighed, mixed, and then added on top of ~0.2246 g of Li_3N inside an alumina crucible (OD: 18mm; ID: 13mm; length: 40cm). 2%H_2O–98%Ar (20 cm^3/min) was fed into the molten salt for 300 minutes at 500 °C.

Table S2. Screenshots of the simulation results for the reactions between the alkaline species (Li_3N, Li_2NH, $LiNH_2$, LiH) with the proton sources (H_2, NH_3, H_2O, HCl) in the respective initial state (IS), the transition state (TS), and the final state (FS). Color code: N atom, blue; H atom, white; Li atom, pink; O atom, red; Cl atom, green. The lines between some atoms are shown mainly to make their relative positions and distances more discernible. Some of the lines do not represent the presence of chemical bonds.

		Li_3N	**Li_2NH**	**$LiNH_2$**	**LiH**
H_2	IS	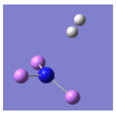	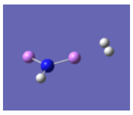	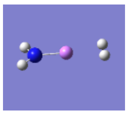	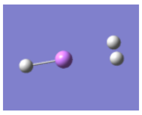
	TS	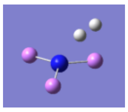	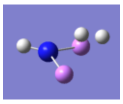	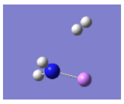	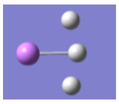
	FS	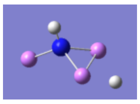	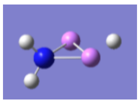	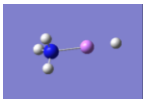	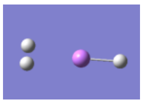
NH_3	IS	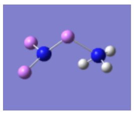	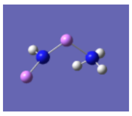	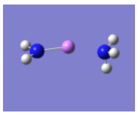	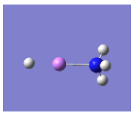
	TS	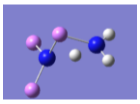	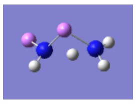	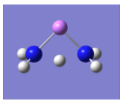	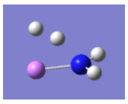
	FS	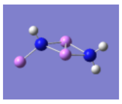	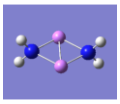	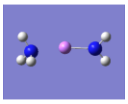	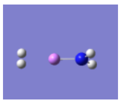
H_2O	IS	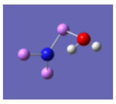	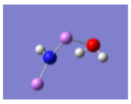	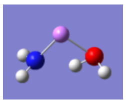	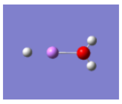
	TS				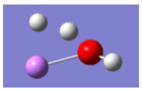
	FS	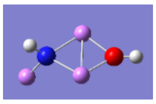	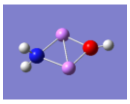	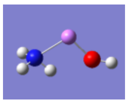	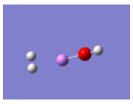
HCl	IS	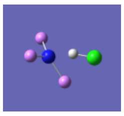	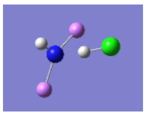	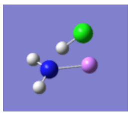	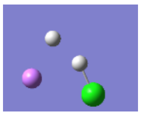
	TS				
	FS	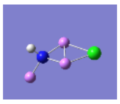	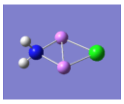	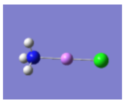	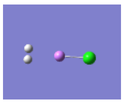

Table S3. The simulation results of different gases with Li_3N, Li_2NH, $LiNH_2$, and LiH. The calculations were performed using Gaussian 09 software [1], with the B3LYP functional and 6-31G(d) basis set.

		Li_3N	Li_2NH	$LiNH_2$	LiH
H_2	TS (eV)	0.01	0.19	0.10	0.60
	FS (eV)	-2.30	-2.40	-0.60	0.00
NH_3	TS (eV)	0.25	0.17	0.34	0.88
	FS (eV)	-2.30	-2.50	-0.00	0.60
H_2O	TS (eV)				0.05
	FS (eV)	-3.08	-3.29	-0.80	-0.48
HCl	TS (eV)				
	FS (eV)	-4.00	-4.04	-2.32	-2.00

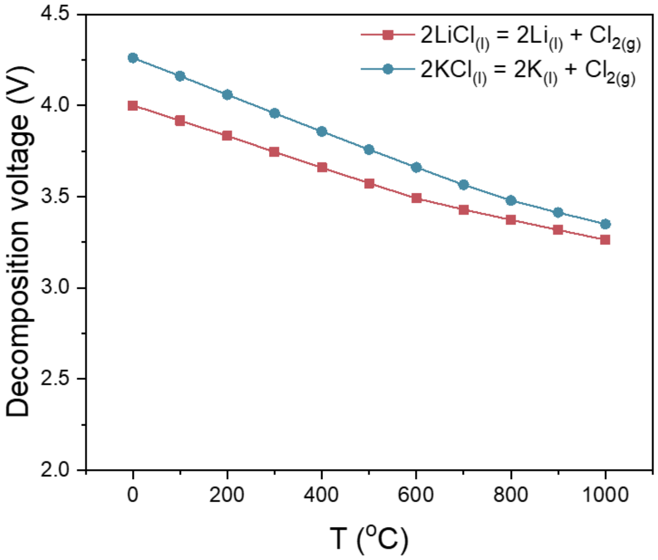

Figure S9. The standard decomposition voltages of molten LiCl and molten KCl as a function of temperature, with data obtained from the HSC Chemistry database.[2]

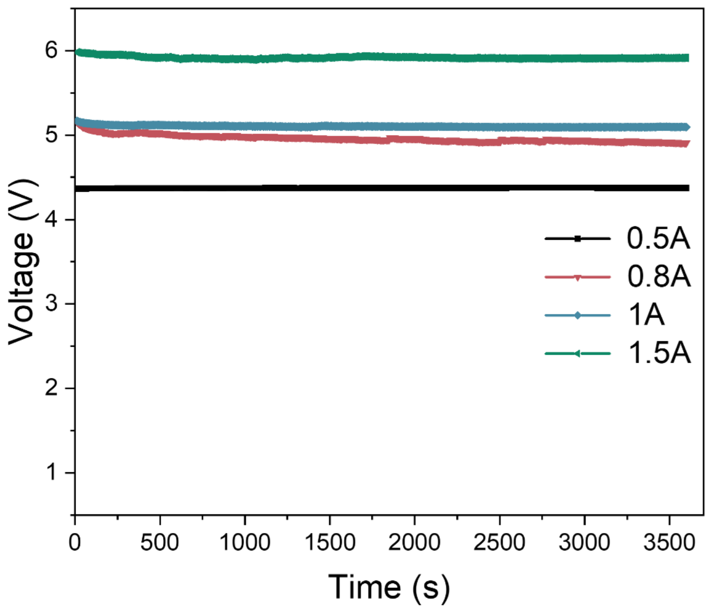

Figure S10. The voltage vs. time data during the constant-current electrolysis scans at different currents using the molten salt electrochemical setup as illustrated in Figure 5a.

Note S1. Calculation of the synthesis efficiency of NH_3

In the 3-step method for NH_3 synthesis in the molten salt-based system, the number of electrons transferred during the 1st step of electrolysis can be used to determine the amount of metallic Li produced assuming a 100% Faradaic efficiency. Assuming that all of this Li can be used for the N_2 fixation, the molar amount of Li_3N can be calculated. If further assuming that all of this Li_3N can be converted into NH_3 by reacting with HCl, the theoretical amount of NH_3 produced can be calculated. In each experiment, the exit gas was passed into H_2SO_4 aqueous solution. The actual amount of NH_3 collected in the H_2SO_4 aqueous solution was determined by coupling a colorimetric indicator method with the UV-Vis spectroscopy. The synthesis efficiency of NH_3 was defined as the ratio of the actual amount of NH_3 collected to the theoretical amount of NH_3 produced (i.e., the theoretical yield of NH_3), as expressed by the following formula:

$$\eta_{NH_3} = n_{NH_3} \ / \ \frac{current * duration * N}{N_A * 3}$$

where:

- η_{NH_3} represents the synthesis efficiency of NH_3,
- n_{NH_3} represents the number of moles of NH_3 collected by the H_2SO_4 aqueous solution,
- *current* represents the electrolysis current,
- *duration* represents the electrolysis duration,
- *N* represents the number of electrons per coulomb,
- N_A represents Avogadro's constant.

If ammonium chloride needs to be considered, the total synthesis efficiency of NH_3 and NH_4Cl (η_{total}) is expressed as follows:

$$\eta_{total} = \eta_{NH_3} + \eta_{NH_4Cl} = [n_{NH_3} + n_{NH_4Cl}] \ / \ \frac{current * duration * N}{N_A * 3}$$

where

- η_{NH_4Cl} represents the synthesis efficiency of NH_4Cl,
- η_{NH_4Cl} represents the moles of NH_4Cl collected near the inner surface of the stainless steel flange.

Table S4. The total amount of NH_3 synthesized and the synthesis efficiency of NH_3 after the three-step experiments involving electrolysis at different currents.

Electrolysis current in the 1st step	Total mass of NH_3 collected (g)	Theoretical amount of NH_3 produced (g)	Synthesis efficiency of NH_3 (%)
0.5 A	0.0090	0.1058	8.48
0.8 A	0.0187	0.1692	11.02
1.0 A	0.0340	0.2115	16.07
1.5 A	0.1545	0.3172	48.68

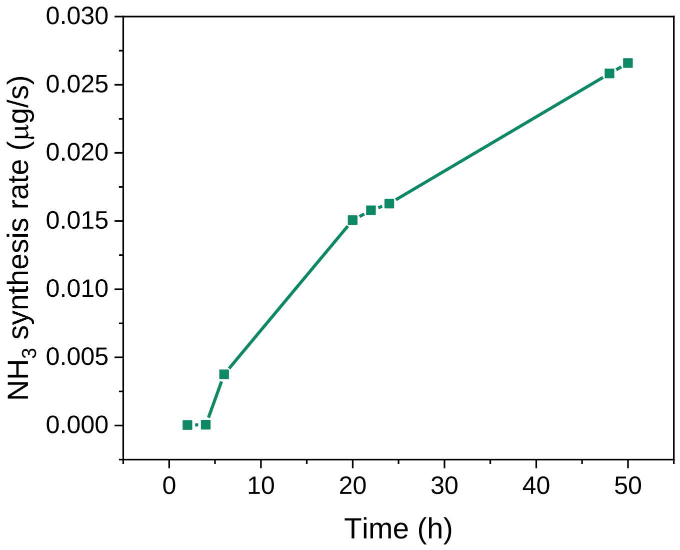

Figure S11. Time dependence of the NH_3 synthesis rate in the three-step experiment involving bubbling a mixture of H_2 (10 cm^3/min) and Ar (10 cm^3/min) in the 3rd step following a 1 h electrolysis at 5 V in the 1st step and a 2 h N_2 feeding to the bottom of the molten salt near the cathode in the 2nd step. Note that the N_2 was fed to the space confined by the alumina sleeve above the molten salt surface during the 1st step, and the N_2 bubbling to the bottom of the molten salt was also maintained during the 3rd step.

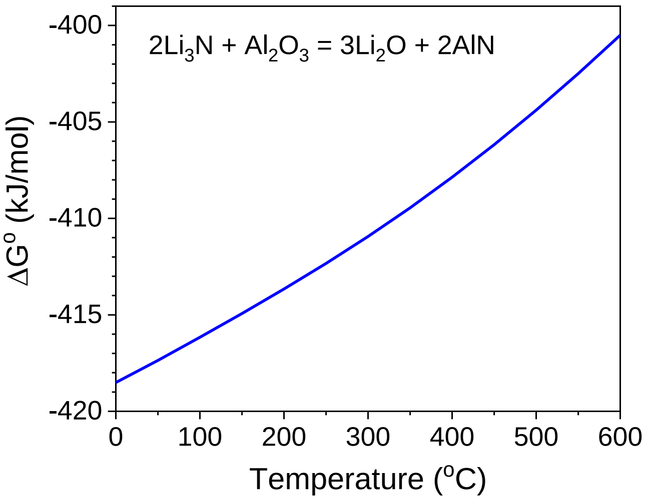

Figure S12. The temperature dependence of the molar standard Gibbs free energy change (ΔG°) for the reaction of $2Li_3N + Al_2O_3 \rightleftharpoons 3Li_2O + 2AlN$. The data were obtained from the HSC Chemistry database.[2] The negative value of ΔG° suggests the thermodynamic spontaneity of the corrosion of Al_2O_3 by Li_3N dissolved in the molten salt.

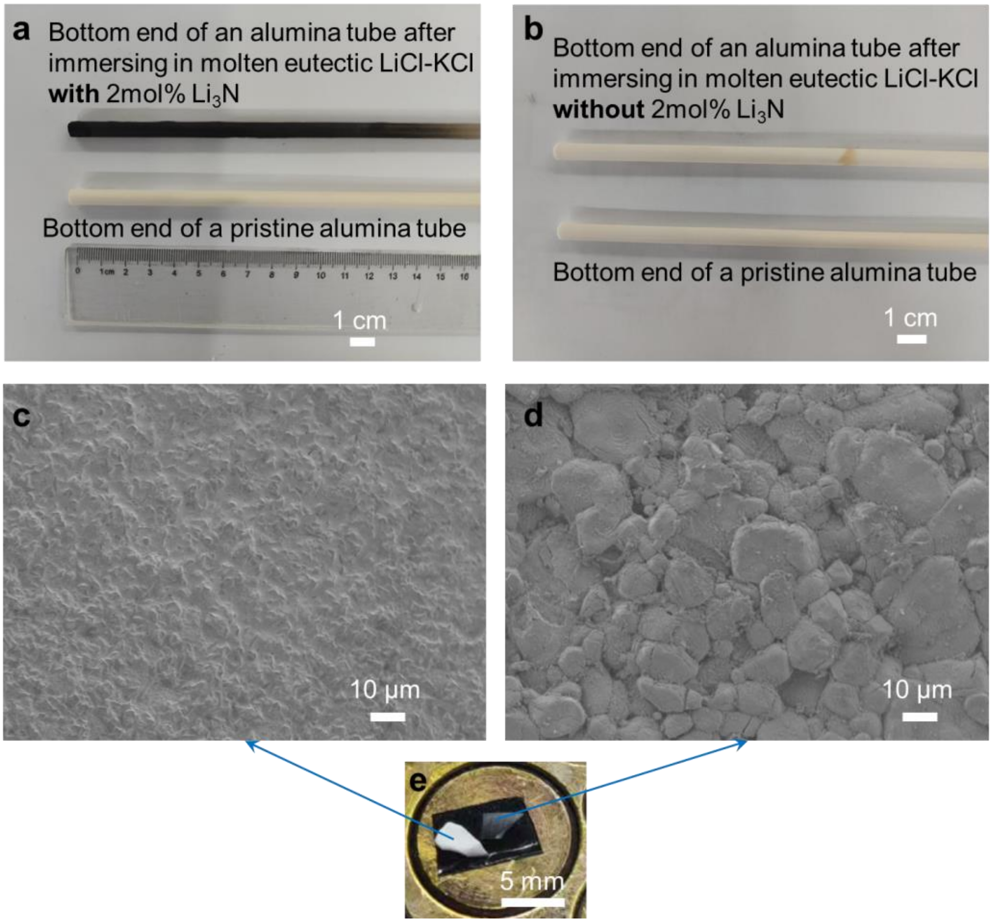

Figure S13. (a) Digital photographs of a pristine alumina tube and an alumina tube after immersing in molten eutectic LiCl–KCl *with* 2mol% Li_3N for 20 h at 500 ºC. The alumina tube turned black after the reaction with Li_3N in the molten salt. (b) Digital photographs of a pristine alumina tube and an alumina tube after immersing in molten eutectic LiCl–KCl *without* Li_3N for 20 h at 500 ºC. The alumina tube after immersing in LiCl–KCl remained white, suggesting the key role of Li_3N in corroding the alumina. (c) SEM image of an inner surface of a piece of alumina sample (white sample in panel *e*) showing smooth morphology. (d) SEM image of the black surface of a piece of alumina sample after immersing in the molten salt containing 2mol% Li_3N (black sample in panel *e*), showing rough morphology and thereby suggesting the corrosion of alumina with Li_3N. (e) Digital photographs of two alumina samples above a carbon conductive tape on a copper holder for SEM characterization.

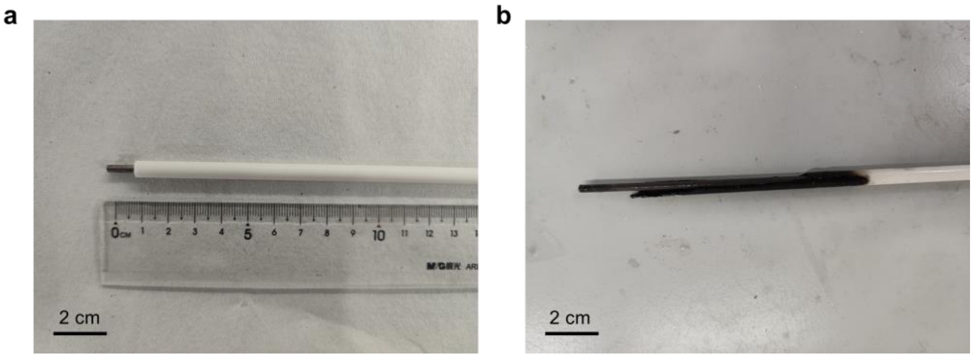

Figure S14. (a) Digital photograph of a pristine alumina tube (outer diameter: 6 mm). Note that the Ni metal rod (diameter: 3 mm) inside the alumina bubbling tube was used as the cathode for the electrolysis. (b) Digital photograph of an alumina tube after the experiment comprising of three cycles and each involving 1 h electrolysis at 1.5 A. The part of the alumina tube submerged in the molten salt was corroded.

References for Supplementary Information

1. P. Chen, Z. Xiong, J. Luo, J. Lin and K. L. Tan, *Nature*, 2002, **420**, 302-304.
2. A. Roine, *HSC Chemistry Database 5.11*, 2002, Outokumpu Research, Finland.